

DESIGN OF A PIN-ON-DISK TRIBOMETER WITH *IN SITU* OPTICAL
PROFILOMETRY

By

JAMES HARLEY KEITH

A THESIS PRESENTED TO THE GRADUATE SCHOOL
OF THE UNIVERSITY OF FLORIDA IN PARTIAL FULFILLMENT
OF THE REQUIREMENTS FOR THE DEGREE OF
MASTER OF SCIENCE

UNIVERSITY OF FLORIDA

2010

© 2010 James Harley Keith

DEDICATION

Here's to you Jesus...one solid dude.

ACKNOWLEDGEMENTS

I would like to thank Dr. Richard Schulz, 'Granddaddy', for taking me fishing for the first time and being a lifelong idol. He was the original mystery meat chef.

I would like to thank Dr. Sarah Schulz, 'SaSa', for her wisdom, patience and financial support through college.

I would like to thank John and Carrie Keith for their continuing support. Thank you for putting up with me and my mess in the driveway.

I would like to thank Mike Braddock for his guidance and enthusiasm.

I would like to thank Misti Keith for her love and support, while I lost sleep over the stresses of this work.

I would like to thank Dr. Greg Sawyer for the adventures over the past three years. He made me a better engineer and taught me to push life to the limits at every opportunity. Granddaddy would have approved.

I would like to thank all of the members of the University of Florida Tribology Lab, current and past for their efforts. Without their hard work to build upon, my success would not have been possible. I would especially like to thank Ira Hill for helping me automate the tribometer in this work.

TABLE OF CONTENTS

	<u>page</u>
ACKNOWLEDGEMENTS	4
LIST OF TABLES.....	6
LIST OF FIGURES.....	7
ABSTRACT	8
CHAPTER	
1 INTRODUCTION	9
2 REVIEW OF LITERATURE	10
Optical Profilometry	10
Wear Rate and Coefficient of Friction.....	11
<i>In Situ</i> Wear Monitoring	11
3 PIN-ON-DISK APPARATUS.....	13
Tribometer	13
Linear Positioning Stages.....	13
Cantilever	14
Capacitance Probes.....	14
Rotary Positioning Stage.....	14
Data Acquisition and User Interface.....	15
Force Measurement.....	15
Optical Profiler	15
4 MEASUREMENT UNCERTAINTY	17
Error Source Analysis.....	17
Mathematical Analysis.....	19
5 TEST RESULTS AND DISCUSSION.....	22
6 CONCLUSION.....	25
APPENDIX	
LIST OF REFERENCES	26
BIOGRAPHICAL SKETCH.....	27

LIST OF TABLES

<u>Table</u>	<u>page</u>
4-1 Measurement uncertainty analysis results	21

LIST OF FIGURES

<u>Figure</u>	<u>page</u>
2-1 Typical microscope based white-light interferometer. [1]	10
3-1 EZ-RoD pin-on-disk tribometer with <i>in situ</i> optical profilometry.....	13
4-1 Capacitance probe target alignment error. a) Target with angular misalignment independent of displacement. b) Displacement dependent angular misalignment.	17
4-2 Component errors of horizontal X axis, EBX: pitch error motion of X, EAX: Roll error motion of X.....	18
4-3 Schematic of the pin-on-disk contact with EYY error. EYY: Position error of the Y axis that offsets the pin from center.	19
5-1 Optical profilometer images of Au 95 wt %, Cu 5 wt % disk before and after sliding contact. The images in the left column are height maps and images in the right column are intensity maps of the a) & b) surface before test, c) & d) after 15 cycles of sliding, e) & f) after 750 cycles of sliding.	22
5-2 Ultra-nano-crystalline-diamond coated sphere on Au 95 wt %, Cu 5 wt % disk. a) Normal and friction force versus cycle number, b) resultant coefficient of friction versus cycle number.	23

Abstract of Thesis Presented to the Graduate School
of the University of Florida in Partial Fulfillment of the
Requirements for the Degree of Master of Science

DESIGN OF A PIN-ON-DISK TRIBOMETER WITH *IN SITU* OPTICAL
PROFILOMETRY

By

James H. Keith

August 2010

Chair: W. G. Sawyer
Major: Mechanical Engineering

A pin-on-disk tribometer with *in situ* optical profilometry was constructed. The tribometer is capable of loads up to 200 mN, 25 revolutions per minute and angular positioning resolution of 50 μ rad. An ultra-nano-crystalline-diamond coated sphere was run on a 95 wt % Au and 5 wt. % Cu disk. Friction results and *in situ* wear track images were presented. Measurement uncertainty analysis was performed for loads typical of the test in this work and was shown to be less than 5%.

CHAPTER 1 INTRODUCTION

Tribology is the study of interacting surfaces in relative motion and encompasses the fields of friction, lubrication and wear. To investigate the reaction of different surfaces in contact, and the governing mechanisms of friction, lubrication and wear, many test apparatuses have been conceived. These tribometers have taken many forms; a common arrangement is the pin-on-disk, where a stationary pin is imposed on a rotating disk. Typically, the apparatus will be instrumented with force or deflection sensors to meter the friction force. Depending on the loading scheme, the normal force may be instrumented as well. This work describes a pin-on-disk tribometer with *in situ* optical profilometry designed for the University of Florida Tribology Lab and analyses its ability to accurately measure normal and friction forces.

CHAPTER 2 REVIEW OF LITERATURE

Optical Profilometry

Optical profilometry is a method of non-contact surface height measurement commonly used to quantify surface roughness. A type of optical profilometry of particular interest to this work is interference microscopy. Interference microscopy combines an interferometer and microscope into one instrument for surface measurement. The objectives are either Michelson, Mirau or Linnik (all being modifications of the Michelson interferometer)[1]. Figure 2-1 depicts the light path of a Mirau interferometer similar to the profilometer used in this work.

The objective is vertically scanned to induce interference fringes on the surface. The fringes are recorded by the charge coupled device and are used to generate a surface height map.

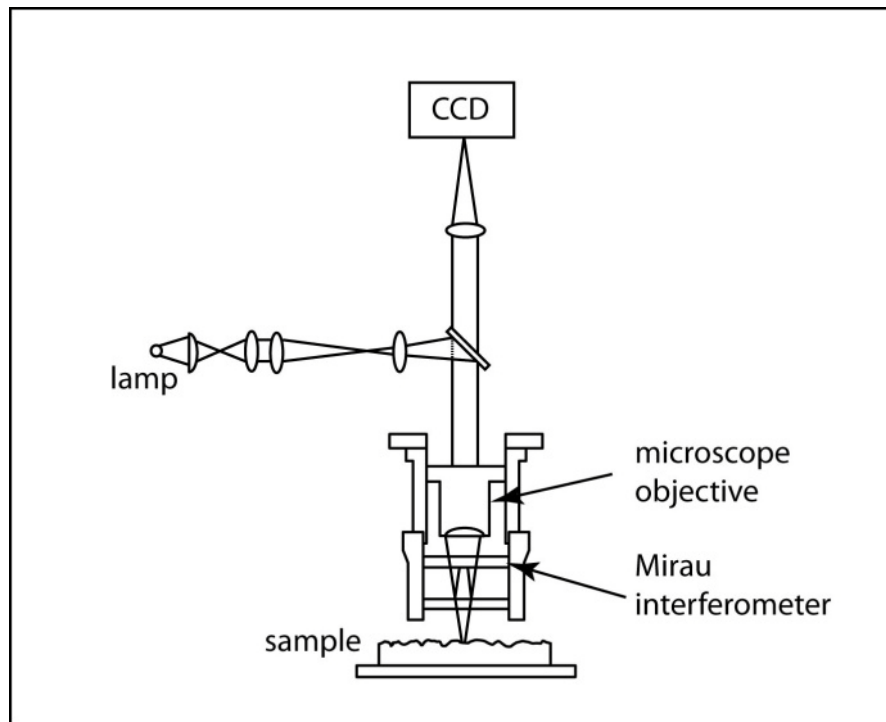


Figure 2-1. Typical microscope based white-light interferometer. [1]

Wear Rate and Coefficient of Friction

Two bodies in contact moving with respect to one another may generate wear debris. J. F. Archard developed the following relationship that aids in the prediction of the rate of material loss to wear (equation 1).

$$W = \frac{KsP}{P_m} \quad (1)$$

Where W is the worn volume, K a dimensionless constant related to the probability of a wear particle, s is the sliding distance, P is the applied load and p_m is the flow pressure of the softer material [2]. A convenient modification of Archard's equation is

$$W = KsP \quad (2)$$

where K is a dimensional constant and the relation does not require knowledge of material flow pressure.

The coefficient of friction, denoted as μ , is the ratio of the friction force on two bodies in contact and the normal force applied to them as seen in equation 3.

$$\mu = \frac{F_f}{F_n} \quad (3)$$

In Situ Wear Monitoring

Wear mechanisms can be complex involving solid mechanic, thermodynamic and chemical phenomenon, among others, and also be transient. For example, a lubricious film could fatigue and delaminate from the substrate after a million loading cycles but show negligible wear up until that point. To label that scenario with one wear rate could be misrepresentative.

Measuring volume loss *in situ* can highlight wear trends that could otherwise be lost in *ex situ* volume loss analysis. Bares *et al* studied copper-on-copper sliding

electrical contacts in a humid copper environment. The tribometer was designed for linear reciprocation with *in situ* scanning white light interferometry. Wear rates were associated with different current densities by measuring volume loss *in situ* [3].

CHAPTER 3 PIN-ON-DISK APPARATUS

Tribometer

The tribometer in this work is a symphony of instruments that are responsible for the loading of two surfaces under prescribed motion to generate friction forces and wear debris while metering the loads, relative motion and wear track evolution.

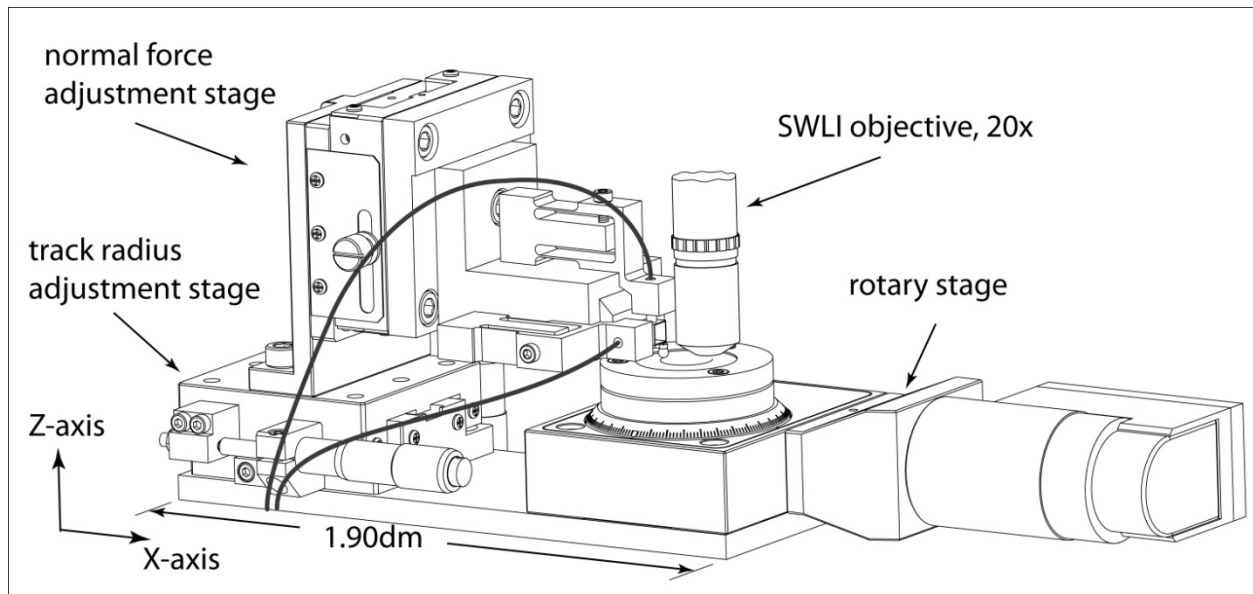


Figure 3-1. EZ-RoD pin-on-disk tribometer with *in situ* optical profilometry.

Linear Positioning Stages

Pin load and track radius are adjusted by two manual, linear ball bearing stages manufactured by OptoSigma (model number 123-0715). The stages are mounted orthogonal to one another and the sample surface. In this configuration, pin position is independently adjustable along the X and Z axes, depicted in Figure 3.1.

The stages are adjusted by manipulation of side mounted micrometers. The micrometers have verniers every $10\mu\text{m}$ of linear translation and position can be interpolated to approximately $3\mu\text{m}$ between the verniers.

Cantilever

The pin is mounted on a flexible member that is referred to as a cantilever. The cantilever selection process suffers from a solid mechanic duality. It must be stiff whilst compliant. Real surfaces are not flat or smooth and, as the disk rotates, the cantilever must be compliant enough to follow the disk's surface, but stiff enough to impart the desired load onto the pin.

For this work, the stiffest cantilever available from CSM instruments was called into service. Cantilever number ST-15 has a 2.367 mN/ μm stiffness in the normal direction and 5.217 mN/ μm stiffness in the friction direction.

Capacitance Probes

Lion Precision Elite 3 mm capacitance probes measure the displacement of the cantilever. They explicitly measure the capacitance between the probe and the target. The change in dielectric constant of the atmosphere is neglected, so the only change in capacitance is from the change in distance between the probe and the target. The range of the capacitance probes used on this tribometer is 100 μm . Combined with the ST-15 cantilever, this tribometer can impart loads up to 200mN.

Rotary Positioning Stage

The disk is fixed to a Physik Instrumente (PI) M-060PD rotary positioning stage that is driven by a PI C-863 Mercury Servo Controller. The stage is driven by a pre-loaded worm gear-reduced direct current servo motor and has a maximum velocity of 90°/sec and a resolution of 50 μrad . The Wyko NT9100 optical profilometer as configured has approximately 50 mm between the work table and the objective focal point, so a criterion for stage selection was stage height. The M-060 series has a height of 29 mm leaving 19 mm of vertical clearance for the sample and sample holder.

Data Acquisition and User Interface

A National Instruments PCI-6221 16 bit data acquisition card was use with LabVIEW to record and organize the voltages from the capacitance probes. Virtual instruments for LabVIEW, that aided in the motion commands for the rotary positioning stage, were provided by Physic Instrumente.

The data acquisition card is set to sample the normal and friction force channels at a rate of 1 kHz. In unison, the angular position of the stage is requested by means of the Physic Instrumente position query virtual instrument. The 1kHz data is averaged every second and stored in a cell next to the angular position of that data acquisition cycle. Due to the overhead of the file save, screen update and other peripheral operations, the code saves at a frequency of just over 10 Hz.

Force Measurement

Friction and normal force are measured via the equipment listed in the previous subsection headings. The forces are calculated by the relations

$$F_n = C_{CLn} C_{CP} V_{\Delta n} \quad (4)$$

$$F_f = C_{CLf} C_{CP} V_{\Delta f} \quad (5)$$

where the subscript 'n' indicates the normal direction and the subscript 'f' indicates the friction direction. C_{CL} is the cantilever constant, C_{CP} is the capacitance probe constant, and V_{Δ} is the change in the output voltage.

Optical Profiler

For surface profile characterization, the tribometer is affixed to the two-axis linear motion table of a Wyko NT9100 Optical Profiler. By coherence scanning interferometry, the NT9100 produces three-dimensional surface maps of the object under test with sub-

nanometer vertical resolution [1]. The NT9100 used in this work is equipped with a 20x Mirau objective and field-of-view (FOV) multipliers of 0.55x, 1x and 2x. The test in this work was performed under the 0.55x FOV multiplier resulting in an 11x magnification. The measurement array is 640 x 480 pixels resulting in an analysis area of 437 μm x 583 μm .

CHAPTER 4 MEASUREMENT UNCERTAINTY

No measurement is without error and the first step towards precision is admitting that there is a problem. The purpose of this chapter is to quantify the error in the force measurements taken by the pin-on-disk tribometer.

Error Source Analysis

The tribometer has errors that stem from the electrical system and the mechanical system. For this analysis, the electrical system includes the capacitance probes and the data acquisition card and the mechanical system includes the cantilever and cantilever alignment with respect to the disk surface.

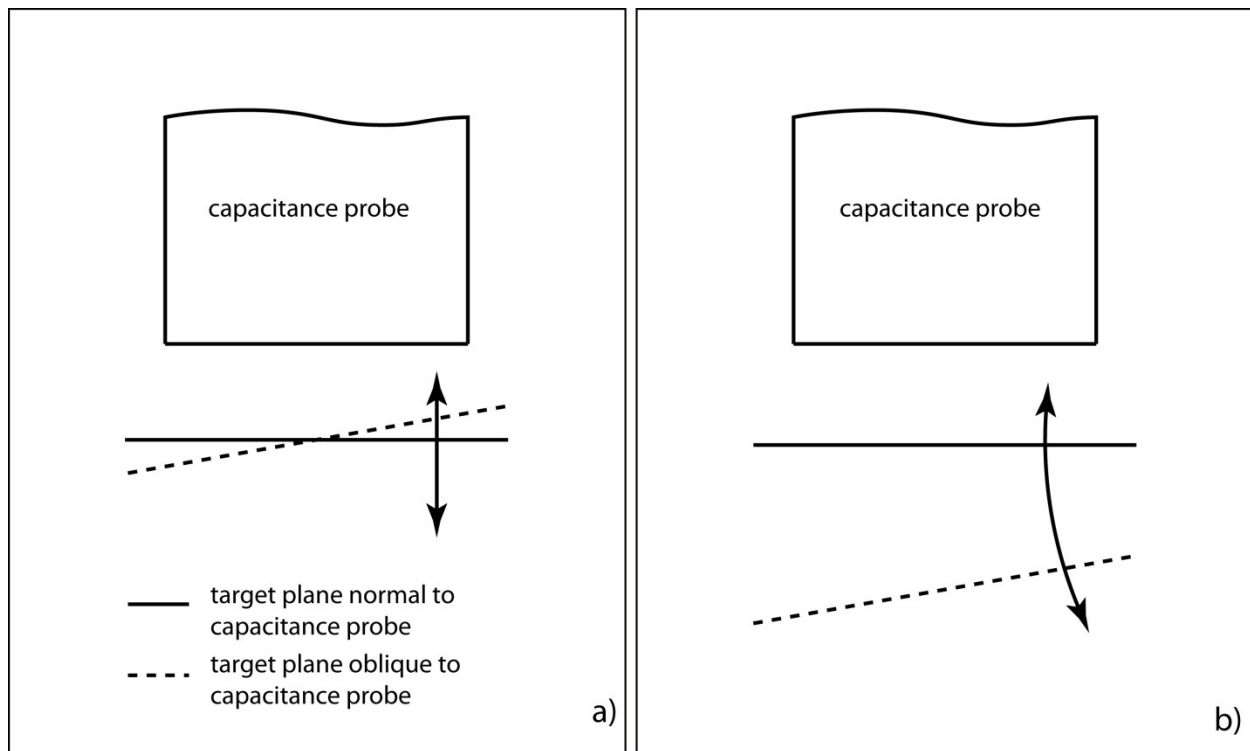


Figure 4-1. Capacitance probe target alignment error. a) Target with angular misalignment independent of displacement. b) Displacement dependent angular misalignment.

The Lion Precision capacitance probes used in this work are capable of measuring distances with a resolution of 15 nm. That resolution is attainable over the 100 μm

range of the probes only if the target translates in an ideal manner. If the target surface is not normal to the measuring face of the capacitance probe as in Figure 4-1-a, the output signal will have an offset suggesting that the probe target is closer than it appears. The tribometer uses a target that is affixed to a cantilever that displaces in an arc. The arc motion imposes a displacement dependent zero offset as depicted in Figure 4-1-b.

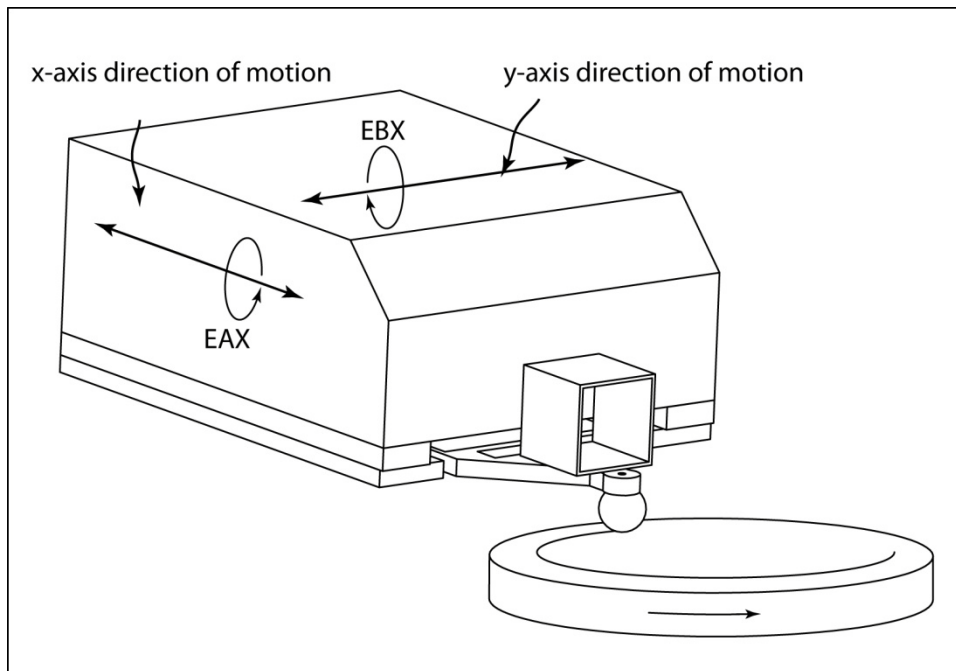


Figure 4-2. Component errors of horizontal X axis, EBX: pitch error motion of X, EAX: Roll error motion of X.

The data acquisition card from National Instruments, used for this tribometer, records analog voltages and stores them as digital voltages in increments of $1/2^n$ where n is the number of bits. The card is capable of 16-bit yielding a voltage increment of approximately $15 \mu\text{V}$.

Manufacturing errors cause misalignment of the measurement axes with respect to the force vectors of interest. The significant contributors of measurement error from

mechanical misalignment were determined to be EAX (roll error motion of X), EBX (pitch error motion of X) and EYY (positioning error) [4]. The first two are depicted in Figure 4-2 and the latter is depicted in Figure 4-3.

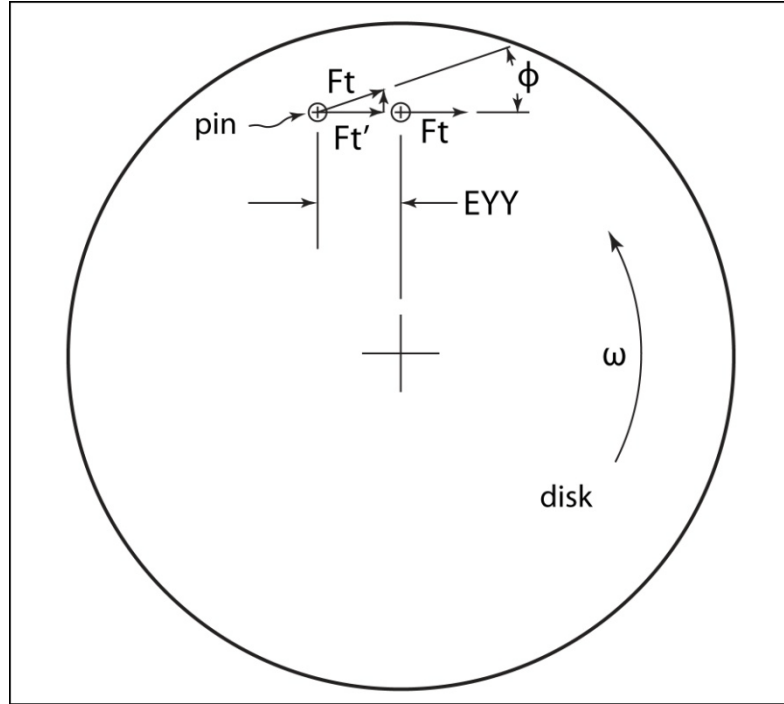


Figure 4-3. Schematic of the pin-on-disk contact with EYY error. EYY: Position error of the Y axis that offsets the pin from center.

Mathematical Analysis

The root sum square method is used for uncertainty analysis of measurements of the contact forces in the normal and friction directions. The root sum square method is as follows:

$$u_R = \left[\left(\frac{\partial R}{\partial x_1} u_1 \right)^2 + \left(\frac{\partial R}{\partial x_2} u_2 \right)^2 + \dots + \left(\frac{\partial R}{\partial x_n} u_n \right)^2 \right]^{1/2} \quad (6)$$

Simply explained, the uncertainty in R is the square root of the sum of the squares of the partial derivative of R with respect to each variable in R multiplied by the uncertainty in the variable.

Applying equation 6 to equation 3, 4 and 5 yields:

$$u_{\mu} = \left[\left(\frac{\partial \mu}{\partial F_n} u_{F_n} \right)^2 + \left(\frac{\partial \mu}{\partial F_f} u_{F_f} \right)^2 \right]^{1/2} \quad (7)$$

$$u_{F_n} = \left[\left(\frac{\partial \mu}{\partial C_{CLn}} u_{C_{CLn}} \right)^2 + \left(\frac{\partial \mu}{\partial C_{CPn}} u_{C_{CPn}} \right)^2 + \left(\frac{\partial \mu}{\partial V_{\Delta n}} u_{V_{\Delta n}} \right)^2 \right]^{1/2} \quad (8)$$

$$u_{F_f} = \left[\left(\frac{\partial \mu}{\partial C_{CLf}} u_{C_{CLf}} \right)^2 + \left(\frac{\partial \mu}{\partial C_{CPf}} u_{C_{CPf}} \right)^2 + \left(\frac{\partial \mu}{\partial V_{\Delta f}} u_{V_{\Delta f}} \right)^2 \right]^{1/2} \quad (9)$$

With these equations, the uncertainty in precision was calculated for the normal force, friction force and coefficient of friction. A nominal value of 50 mN was considered for the normal force and a nominal value of 15 mN was considered for the friction force. The normal force is typical for the test mentioned in this work and the friction force is a worst-case friction value from said test. A high value of friction force would maximize the capacitance probe error, the largest contributor of measurement error.

To appreciate the total uncertainty, bias errors are added to the precision errors with the same root sum square method and are represented as:

$$u_T = \left[u_P^2 + u_B^2 \right]^{1/2} \quad (10)$$

where the bias errors generate from the geometric errors depicted in figure 4-2 and 4-3.

The total calculated uncertainty for the friction force measurement, normal force measurement and coefficient of friction calculation are presented in Table 4-1 below.

Table 4-1. Measurement uncertainty analysis results

Measurand	Nominal Value	Uncertainty
F_n	50 mN	± 1.12
F_f	15 mN	± 0.30
μ	0.3	± 0.01

As tabulated, all of the calculated uncertainties are under 5 %. The largest contributor to uncertainty is the cantilever stiffness coefficient provided by CSM instruments.

CHAPTER 5 TEST RESULTS AND DISCUSSION

A wear test was run on the pin-on-disk tribometer. The pin was loaded against the disk at a nominal load of 50 mN and slid relative to the disk at a velocity of 30 degrees per second or 5 revolutions per minute. After every 360 degrees of revolution, the stage was stopped to image the wear track. This was performed for 750 cycles. Figure 5-1 shows height map and intensity map images. Images c) and d) are after 15 cycles of sliding when the first wear scar appears. Substantial plastic deformation can be seen in images e) and f).

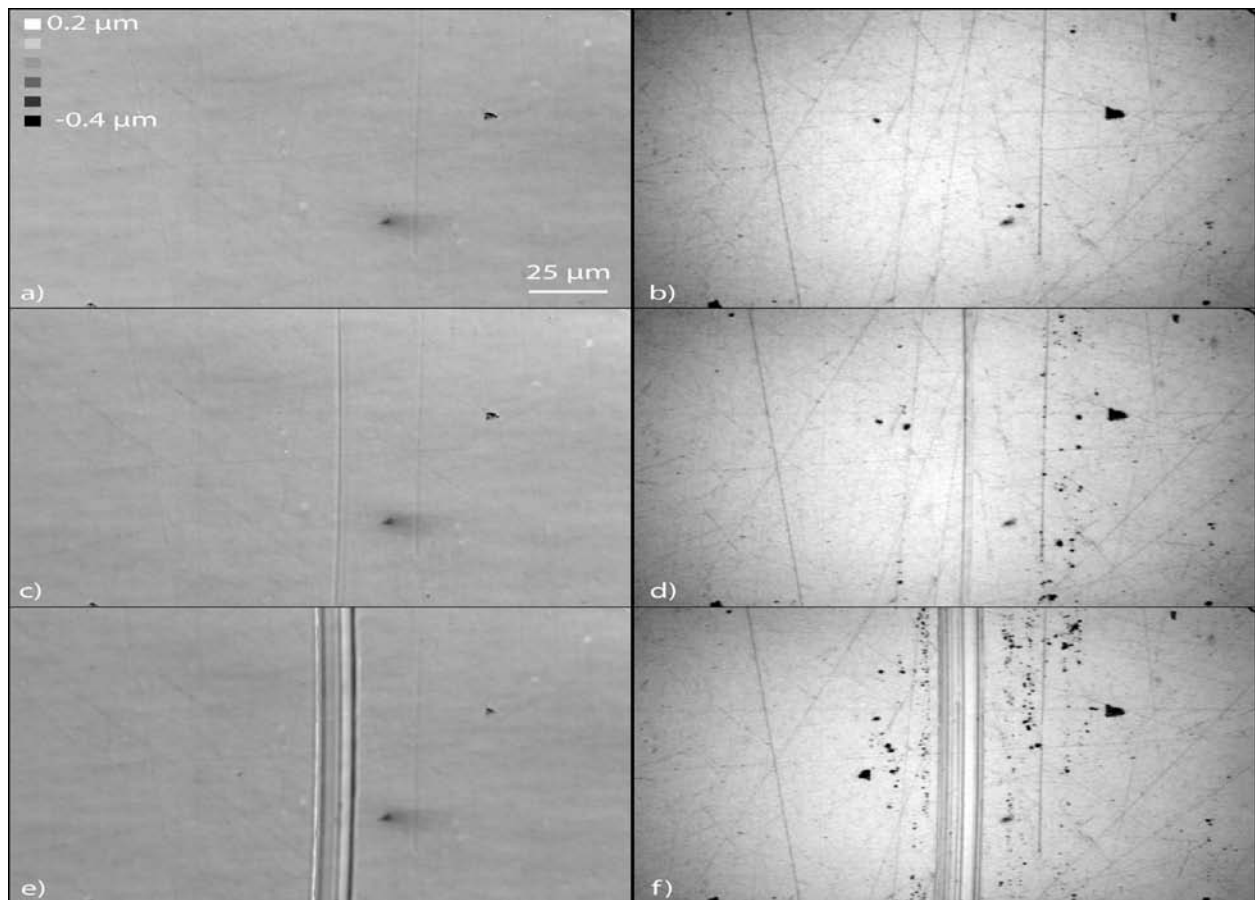


Figure 5-1. Optical profilometer images of Au 95 wt %, Cu 5 wt % disk before and after sliding contact. The images in the left column are height maps and images in the right column are intensity maps of the a) & b) surface before test, c) & d) after 15 cycles of sliding, e) & f) after 750 cycles of sliding.

The normal force and friction force are plotted against cycle number in Figure 5-1a and the resultant coefficient of friction is plotted in Figure 5-1b.

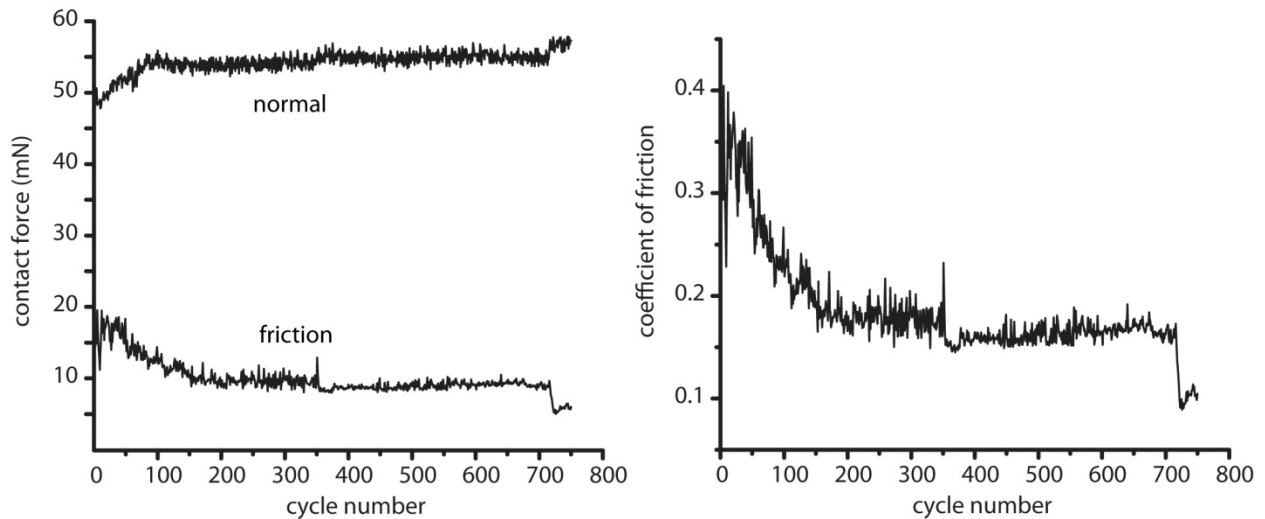


Figure 5-2. Ultra-nano-crystalline-diamond coated sphere on Au 95 wt %, Cu 5 wt % disk. a) Normal and friction force versus cycle number, b) resultant coefficient of friction versus cycle number.

As mentioned in Chapter 2, the tribometer is configured to save angularly resolved friction forces. The data plots in Figure 5-2 are from measurements taken at a unique angular location of 180 degrees of stage rotation. This location was chosen as it is under the objective of the profilometer when the stage is at rest.

In Figure 5-2-a, the normal force is plotted with respect to the cycle number. In the first 100 cycles of the test, the load ramps from just under 50 mN to approximately 55 mN. It seems that the fluctuation in load is a product of thermal expansion. Friction in the worm gear and resistance in the motor are likely sources of heating. To verify the hypothesis of transient temperatures the stage was fitted with a thermocouple in subsequent friction tests. After starting a friction experiment, the temperature displayed on the thermocouple reader would raise about 5 °C. In-test force fluctuation was minimized in subsequent tests by commanding a stage rotation of approximately 80

revolutions at 25 rpm before the friction test was begun. This quickly raised the temperature of the stage to the steady state operating temperature that 5 rpm would produce. Further rotation of the stage at 25 rpm would overheat the stage causing the normal force to decrease during the test until the steady state temperature was reached. The step increase in force at approximately 700 revolutions in Figure 5-2-a was due to the building air conditioning shutting down for Christmas break.

As mentioned in Chapter 2, the sensitivity of adjustment for the manual stages is 50 μm per revolution, allowing for an accurate linear movement of approximately 3 μm by interpolating between verniers. However, the smallest move between stick-slip intervals of the micrometer head seems to be on the order of 1 μm . For this work, the cantilever stiffness was 2.376 mN/ μm . Thus, the smallest single adjustment possible was in excess of 2 mN. After multiple attempts, the stage could usually be adjusted to a desired force value within 1 mN.

CHAPTER 6 CONCLUSION

A pin-on-disk tribometer with *in situ* optical profilometry was built for the University of Florida Tribology Lab. The uncertainty was calculated. The applied normal force has shown to drift approximately 1 μm per $^{\circ}\text{C}$ in temperature change of the rotary stage. Although this effect can be partially mitigated by bringing the rotary stage up to temperature before the test, a more precise fix would be to add an active normal force stage with feedback. The tribometer would, of course, need to be renamed from EZ-RoD to Hard-RoD.

LIST OF REFERENCES

- [1] A.G. Olszak, J. Schmit, M.G Heaton, Interferometry: Technology and Applications. (2001). *Veeco Metrology Group*. Retrieved Dec. 24, 2009, from <http://www.veeco.com>
- [2] J.F. Archard, W. Hirst, The wear of metals under unlubricated conditions, Proc. Royal Soc. of London. Ser. A, Mathematical and Physical Sciences, 236 (1956) 397-410.
- [3] J.A. Bares, N. Argibay, N. Manutler, G.J. Dudder, S.S. Perry, G.R Bourne, W.G. Sawyer, High current density copper-on-copper sliding electrical contacts at low sliding velocities, *Wear* 267(2009) 417-424.
- [4] H. Schwenke, W. Knapp, H. Haitjema, A. Weckenmann, R. Schmitt, F. Delbressine, Geometric error measurement and compensation of machines – An update, *CIRP Annals – Manufacturing Technology* 57 (2008) 660-675.

BIOGRAPHICAL SKETCH

The author is a lifelong Florida resident. His interests in mechanical engineering were first realized in high school when he was working on trucks and Jeeps in his parent's driveway. In pursuit of a mechanical engineering degree, he received an Associate of Arts from Okaloosa Walton Community College in Niceville, Florida in 2003. He received a Bachelor of Science in mechanical engineering from the University of Florida in 2007. He married the love of his life, now Misti A. Keith, that following summer.